

Direct Hydraulic Parameter and Function Estimation for Diverse Soil Types Under Infiltration and Evaporation

Jianying Jiao¹ · Ye Zhang¹ · Jianting Zhu²

Received: 14 January 2016 / Accepted: 21 November 2016 / Published online: 9 December 2016
© Springer Science+Business Media Dordrecht 2016

Abstract A new computationally efficient direct method is applied to estimating unsaturated hydraulic properties during steady-state infiltration and evaporation at soil surface. For different soil types with homogeneous and layered heterogeneity, soil hydraulic parameters and unsaturated conductivities are estimated. Unlike the traditional indirect inversion method, the direct method does not require forward simulations to assess the measurement-to-model fit; thus, the knowledge of model boundary conditions (BC) is not required. Instead, the method employs a set of local approximate solutions to impose continuity of pressure head and soil water fluxes throughout the inversion domain, while measurements act to condition these solutions. Given sufficient measurements, it yields a well-posed system of nonlinear equations that can be solved with optimization in a single step and is thus computationally efficient. For both Gardner's and van Genuchten's soil water models, unsaturated hydraulic conductivities and pressure heads (including the unknown BC) can be accurately recovered. When increasing measurement errors are imposed, inversion becomes less accurate, but the solution is stable, i.e., estimation errors remain bounded. Moreover, when the unsaturated conductivity model is known, inversion can recover its parameters; if it is unknown, inversion can recover a nonparametric, piecewise continuous function to which soil parameters can be obtained via fitting. Overall, inversion accuracy of the direct method is influenced by (1) measurement density and errors; (2) rate of infiltration or evaporation; (3) variation of the unsaturated conductivity; (4) flow direction; (5) the number of soil layers.

Keywords Inverse method · Direct method · Hydraulic conductivity · Unsaturated flow

✉ Jianying Jiao
jjiao1@uwyo.edu

¹ Department of Geology and Geophysics, University of Wyoming, Laramie, WY, USA

² Department of Civil and Architectural Engineering, University of Wyoming, Laramie, WY, USA

1 Introduction

Simulation of flow through unsaturated soils requires accurate knowledge of the soil hydraulic properties, namely the water retention function and the unsaturated hydraulic conductivity. A variety of laboratory and field methods exist to estimate these highly nonlinear soil hydraulic functions. A review with a discussion of the relative advantages and limitations of the different methods can be found in [Dirksen \(2000\)](#), [Durner and Lipsius \(2005\)](#), among others. Due to sampling “support effect,” spatial correlation of soil hydraulic parameters, and non-representativeness of the laboratory flow conditions, soil properties obtained from laboratory experiments using small cores are often inadequate for simulating unsaturated flow dynamics at field or larger scales ([Mertens et al. 2005](#)). Though field-based testing methods have also been developed to estimate these properties under in situ conditions (e.g., [Zhang et al. 2003](#)), such methods tend to be range restrictive, time-consuming, and expensive to implement. Another approach is to use inverse modeling to estimate the coupled soil water retention and unsaturated hydraulic conductivity functions ([Vrugt et al. 2008](#); [Dai et al. 2008](#)). In general, inverse methods are developed using parameter estimation techniques, often under controlled conditions by imposing well-defined soil water pressure boundary conditions, thereby inducing outflow (e.g., [Nasta et al. 2011](#)).

One of the most popular applications of the inverse solution techniques to estimate hydraulic properties of unsaturated soils in the laboratory is the one-dimensional (1D) column test. Three types of methodologies exist ([To-Viet et al. 2013](#)): one-step outflow experiments (instantaneous application of one large pressure step), multi-step outflow experiments (application of several, sequentially smaller pressure steps), and continuous flow experiments (application of a continuous change in pressure gradient). These experiments are performed under steady-state or transient flow conditions which can also include wetting or drying cycles. The hydraulic properties of the unsaturated soils are determined using numerical methods based on the measured discharge water velocity as well as the evolution of soil suction and water content during the test. With these methods, the unknown parameters of the hydraulic properties are estimated by minimizing the difference between the predicted and observed measurements of flow rate, water content, and soil suction. The application of inversion to one-step outflow experiments was proposed early to estimate hydraulic properties using cumulative outflow data ([Kool et al. 1985a, b](#); [Kool and Parker 1988](#)).

In estimating soil hydraulic parameters, inverse methods are typically based upon the minimization of a suitable objective function, which expresses the discrepancy between the observed values and the predicted system responses using a model. Estimation for the hydraulic property functions and parameters is usually accomplished with an indirect approach of parameter optimization. For example, soil hydraulic properties are commonly assumed to be described by an analytical model with unknown parameter values. The system response is represented by a numerical or analytical solution of the unsaturated flow equation in conjunction with the parameterized hydraulic functions and suitable initial and boundary conditions (BC), which are assumed fully known. Using parameter search algorithms (e.g., [Metropolis et al. 1953](#); [Hastings 1970](#); [Vrugt et al. 2008](#); [Ines and Mohanty 2008](#); [Shin et al. 2013](#); [Carrera and Neuman 1986](#); [Sun 1994](#); [Dai and Samper 2004](#); [Ye et al. 2005](#); [Yang et al. 2014](#)), initial estimates of the hydraulic parameters are iteratively improved by minimizing the objective function until a desired degree of precision or convergence is obtained. With the indirect approach, both parameter spatial distribution and their correlations can be assessed. However, because soils consist of complex materials and flow boundary conditions, which, for the simulation of the flow process, are often unknown or uncertain in the field,

indirect inversion of the hydraulic properties often leads to nonunique solutions (Levasseur et al. 2009). To overcome this problem in estimating the hydraulic property functions, inversion using a combination of time-dependent outflow, water content, and capillary pressure measurements has been proposed (Durner et al. 1997). Numerous methods have also been developed to include additional components, such as water content (Van Dam et al. 1992; Bohne et al. 1993; Simunek et al. 1998) or capillary pressures (Toorman et al. 1992; Eching and Hopmans 1993), into the objective function formulation for optimization (Crescimanno and Iovino 1995).

In this study, we develop a direct and efficient inversion approach for estimating soil hydraulic properties under steady-state infiltration or evaporation where field BC are unknown. Such a limitation precludes the development of a forward numerical/analytical model with which measurement-to-model fit can be evaluated via objective functions. For saturated flow problems, various earlier approaches of direct methods were developed. For example, in the comparison model method (Ponzini and Crosta 1988; Pasquier and Marcotte 2006), the steady-state groundwater flow equation is discretized using the finite-difference method, while to solve the inversion their approach requires the knowledge of aquifer boundary conditions. The differential system method (Vassena et al. 2007) is also a type of direct approach that is based on the method of fundamental solutions (MFS) (Fairweather and Karageorghis 1998). Boundary conditions are again required. In Brouwer et al. 2008, the direct method must be combined with two separate forward simulations requiring boundary conditions. Moreover, as discussed in the review by Zhou et al. (2014), most of the existing direct methods suffer from the need to require exhaustive measurements, which are often obtained from interpolating point measurements. Clearly errors can be introduced into inversion depending on the interpolating algorithms used. In the method we are introducing here, boundary conditions are not required, nor do we use any interpolation on measurements. Instead, any boundary conditions are treated as conditioning measurements. Unlike the earlier direct methods, our new approach can simultaneously estimate soil hydraulic properties and state variables (pressure head profile and fluxes) from which the field BC can be inferred. Thus, the direct method obviates one source of nonuniqueness that can arise from making BC assumptions. Also, indirect inversion, when combined with optimization, can be computationally intensive, as the forward model needs to be run many times. In comparison, only one inversion system of equation is assembled and solved with the direct method; thus, it is computationally efficient. Moreover, indirect approaches require parameterizing a specific soil hydraulic property model a priori in order to run the forward model during optimization. However, incorrect assumption of this model may contribute to the “structure errors” during inversion. For example, actual soil properties at a field site could be well approximated by the van Genuchten’s model (Van Genuchten 1980), but modeler may choose to optimize parameters of the Gardner’s model (Gardner 1958). The new direct method can infer the soil hydraulic model without making a priori assumption.

The direct method has been successfully implemented in inverting a variety of saturated flow problems (Irsa and Zhang 2012; Jiao and Zhang 2014a, b, 2015a, b, 2016; Zhang et al. 2014). This study extends this technique to inverting one-dimensional (1D) unsaturated flow under unknown BC for a variety of soil types under infiltration or evaporation. The direct method, similar to other inversion approaches, requires appropriate measurements of sufficient quantity and quality, while its results are influenced by parameterization. Because it does not solve the forward model, an “inversion grid” can employ flexible discretization. A variety of parameterizations, ranging from zoned to highly parameterized, can be used, which influence data requirement as well as inversion quality. The direct method can also be integrated with geostatistics to quantify uncertainty in the estimated parameters and BC (Jiao

and Zhang 2015b). Such an analysis, however, is not the focus here. Finally, the proposed inversion of unsaturated flow uses pressure heads and soil water fluxes for homogeneous or layered media. As long as appropriate conditions are met yielding these measurements, both laboratory and field data can be analyzed.

In the following sections, a forward model, which is developed to test the proposed inversion approach, is introduced first. The principle of direct inversion and its solution technique are then presented. By inverting infiltration and evaporation in soils with homogeneous or layered configuration, accuracy and stability of the direct method are demonstrated. Assuming that soil hydraulic properties can be described by either the Gardner's or the van Genuchten's model, measurement density, measurement error, domain length scale, and BC are systematically varied in inversion. The effect of each variation on the quality of inversion is examined. Results and insights of this study are presented and discussed, along with future research directions.

2 Theory

2.1 The Forward Problem

Under one-dimensional steady-state infiltration or evaporation in the vadose zone, the water conservation equation without source/sink terms can be expressed as:

$$\frac{\partial}{\partial z}(q) = 0 \quad \text{on } \Omega \quad (1)$$

and Darcy's Law as:

$$q = -K(\psi) \left(\frac{\partial \psi}{\partial z} + 1 \right) \quad \text{on } \Omega \quad (2)$$

where q is vertical Darcy flux or infiltration rate (positive upward and negative downward) [L/T], and z is vertical distance (positive upward) [L], with $z = 0$ set at the water table. Ω is the forward model domain, which is identical with the inversion domain, $K(\psi)$ is the unsaturated hydraulic conductivity [L/T], and ψ is the pressure head (negative in the unsaturated zone) [L].

In this work, the unsaturated hydraulic conductivity is assumed to follow either the Gardner's model (Gardner 1958) or the van Genuchten's model (Van Genuchten 1980), which can be expressed below as:

$$K(\psi) = K_s \exp(\alpha \psi) \quad (3)$$

or,

$$K(\psi) = K_s \frac{\left\{ 1 - (\beta \psi)^{n-1} [1 + (\beta \psi)^n]^{-m} \right\}^2}{[1 + (\beta \psi)^n]^{m/2}}, \quad m = 1 - \frac{1}{n} \quad (4)$$

where K_s is the saturated hydraulic conductivity [L/T], α (of Gardner's, [$1/L$]) is the rate of reduction in unsaturated hydraulic conductivity with decreasing pressure head, β [$1/L$], m [$-$], and n [$-$] (of van Genuchten's) are the soil-water retention parameters. K_s , β , m , and n can vary in the vertical direction, representing potentially layered soil formations for real-world applications.

Equations (1) and (2) can be solved using finite-difference method (FDM) for which model boundary conditions (BC) are specified as:

$$\psi = g(z) \text{ on } \Gamma \tag{5}$$

where Γ is a Dirichlet-type domain boundary and $g(z)$ describes a set of prescribed pressure heads on Γ . Note that although Dirichlet-type BC are adopted here, other BC types can also be used in the forward model. To test the quality of inversion, the forward model is solved for different soil types under infiltration or evaporation, yielding a set of synthetic problems or reference models. The forward model is solved with the finite-difference method with a finely discretized domain; thus, flow physics is captured in detail from which observations of the state variables are sampled. These observations, error-free or imposed with uniform measurement errors, will be provided to inversion for both parameter and state variable estimation.

2.2 The Inverse Problem

In the direct inversion method, three sets of constraints are enforced: (1) Via the development of approximate solutions (i.e., fundamental solutions for inversion), global continuity of the pressure head and Darcy flux is imposed throughout the solution domain Ω ; (2) local conditioning of the fundamental solutions to observed pressure heads and fluxes; (3) an equation constraint imposing flow physics at selected spatial positions in Ω . The continuity constraints can be written as:

$$\int R_\psi(x) \delta(x - p_j) dx = 0, \quad j = 1, \dots, Y \tag{6}$$

$$\int R_q(x) \delta(x - p_j) dx = 0, \quad j = 1, \dots, Y \tag{7}$$

where $R_\psi(x)$ and $R_q(x)$ are residuals of the approximating functions of pressure head and Darcy flux at the j th cell interface in the inversion grid, respectively. Y is the total number of cell interfaces. $\delta(x - p_j)$ is a weighting function which samples the residuals at a set of collocation points p_j on Γ_j . For 1D inversion, only one collocation point is needed on each cell interface. Both residual equations can be expressed as:

$$R_\psi(x) = \psi^i(x) - \psi^k(x) \tag{8}$$

$$R_q(x) = q^i(x) - q^k(x) \tag{9}$$

where ψ and q are a set of proposed fundamental solutions for inversion (next), and i and k denote cells in the inversion grid adjacent to each interface Γ_j .

The fundamental solutions are conditioned at a set of measurement locations:

$$\delta(p_a) (\psi(p_a) - h_a^0) = 0 \quad a = 1, \dots, A \tag{10}$$

$$\delta(p_b) (q_z(p_b) - q_b^0) = 0 \quad b = 1, \dots, B \tag{11}$$

where p_a and p_b are measurement points, h_a^0 , q_b^0 are observed pressure head and flux, respectively, A and B are the total number of measured pressure heads and fluxes, respectively, $\delta(p_a)$ and $\delta(p_b)$ are the weighting functions assigned to the equations to reflect the magnitude of measurement errors. $\delta(p_a)$ and $\delta(p_b)$ are generally proportional to the inverse of the error variance (Hill and Tiedeman 2007). In this study, inversion under both error-free and uniform measurement errors is investigated to evaluate the accuracy and instability of the outcomes with increasing data errors.

To enforce the flow constraints, a third group of equations are developed:

$$\delta(p_c) R_c = 0 \tag{12}$$

where $R_c = \left[\frac{\partial}{\partial z} \left(K(\psi) \left(\frac{\partial \psi}{\partial z} + 1 \right) \right) \right]_c$, $c = 1, \dots, Y + A + B$, where p_c include both the collocation points and the measurement locations, and R_c is residual of the flow equation [Eq. (1)] at p_c . Equations (6) and (7) are written at all Y interfaces in the inversion grid. Equations (10) and (11) are written at the locations where measurements are available. Equation (12) imposes the flow constraints at both the collocation points and the measurement locations. Note that earlier inversion for saturated flow had used local analytical solutions as the fundamental solutions, for which Eq. (12) becomes trivial. However, for soil water problems where the physics is strongly nonlinear, local approximate solutions are used for which Eq. (12) is needed to ensure the correct flow physics.

2.3 Fundamental Solutions

For an individual inversion grid cell (Ω_i), Eqs. (1) and (2) can be written as:

$$\frac{\partial}{\partial z} (q) = 0 \quad \text{on } \Omega_i \tag{13}$$

$$q = -K(\psi) \left(\frac{\partial \psi}{\partial z} + 1 \right) \quad \text{on } \Omega_i \tag{14}$$

where $K(\psi)$ can be expressed by either Eqs. (3) or (4). However, Ω_i is assumed to have homogeneous soil properties for which K_s , α (of Gardner’s model), β , m , and n (of van Genuchten’s model) are constant soil hydraulic parameters. To define heterogeneity, these parameters can vary among the inversion grid cells which together constitute the solution domain.

For the Gardner’s model, local approximate solutions of the pressure head and unsaturated hydraulic conductivity are proposed as:

$$\psi(z) = a_1 + a_2z + a_3z^2 \quad \text{on } \Omega_i \tag{15}$$

$$K(z) = \exp(k_s) \exp(\alpha(a_1 + a_2z + a_3z^2)) \quad \text{on } \Omega_i \tag{16}$$

where $a_1, a_2, a_3, K_s = \exp(k_s)$, and α are the unknown coefficients which will be estimated in inversion. Note that according to the Gardner’s model, $K(\psi) = \exp(k_s) \exp(\alpha\psi)$ and because ψ is proposed as a function of z under steady-state flow, the unsaturated conductivity becomes a function of K_s and z . Equation (16) thus serves to approximate the behavior of K with respect to z and K_s . Using Darcy’s law, the Darcy flux can then be approximated as:

$$q(z) = -\exp(k_s) \exp(\alpha(a_1 + a_2z + a_3z^2)) (a_2 + 2a_3z + 1) \quad \text{on } \Omega_i \tag{17}$$

Together, Eqs. (15), (16), and (17) constitute a set of local approximation solutions (LAS) of inversion, and Eq. (12) must be imposed to ensure flow physics in the solution domain. Given the above expressions, Eq. (12) can then be rewritten as:

$$\begin{aligned} &\delta(p_c) \alpha (a_2 + 2a_3z) \exp(k_s) \exp(\alpha(a_1 + a_2z + a_3z^2)) (a_2 + 2a_3z + 1) \\ &+ \exp(k_s) \exp(\alpha(a_1 + a_2z + a_3z^2)) (2a_3) = 0 \quad \text{on } \Omega_i \end{aligned} \tag{18}$$

Equations (13) and (14) are discretized over the inversion domain, and the above coefficients become cellwise constants: $\mathbf{x}^T = [a_1^l, a_2^l, a_3^l, k_s^r, \alpha^r]$, $l = 1, \dots, M$ (number of inversion grid

cells), $r = 1, \dots, R$ (number of soil layers), where \mathbf{x} is the inverse solution, and superscript T denotes transpose. Layer location is assumed known in inversion.

For the van Genuchten’s model, the unsaturated conductivity is more strongly nonlinear compared to the Gardner’s model, and the coefficients (k_s, β, m, n) are more difficult to obtain. A different set of fundamental solutions of the pressure head and unsaturated hydraulic conductivity is proposed:

$$\psi(z) = b_1 + b_2z + b_3z^2 \quad \text{on } \Omega_i \tag{19}$$

$$K(z) = \exp(b_4 + b_5z + b_6z^2) \quad \text{on } \Omega_i \tag{20}$$

where $b_1, b_2, b_3, b_4, b_5,$ and b_6 are the unknown coefficients which will be estimated in inversion. Note that the contribution of saturated conductivity to $K(\psi)$ is included in the coefficients $(b_4 - b_6)$, which differs from the formulation of Eq. (16). Using Darcy’s law, the Darcy flux can then be approximated as:

$$q_z(z) = -\exp(b_4 + b_5z + b_6z^2) (b_2 + 2b_3z + 1) \quad \text{on } \Omega_i \tag{21}$$

Given Eqs. (19), (20), and (21), all of them LAS, Eq. (12) can be rewritten as:

$$\begin{aligned} \delta(p_c) (b_5 + 2b_6z) (b_2 + 2b_3z + 1) \exp(b_4 + b_5z + b_6z^2) \\ + \exp(b_4 + b_5z + b_6z^2) (2b_3) = 0 \quad \text{on } \Omega_i \end{aligned} \tag{22}$$

For the van Genuchten’s model, Eqs. (13) and (14) are also discretized over the inversion domain and the new set of coefficients are cellwise constants to create a new inverse solution: $\mathbf{x}^T = [b_1^l, b_2^l, b_3^l, b_4^l, b_5^l, b_6^l], l = 1, \dots, M$ (number of grid cells).

2.4 Solution Techniques

By substituting in the LAS (one set of solutions proposed for each unsaturated conductivity model), Eqs. (6)–(12) are assembled to form a system of equations which can be under-determined, exact, or over-determined:

$$f_i(\mathbf{x}) = 0, i = 1, \dots, w \tag{23}$$

where \mathbf{x} is the inverse solution, $f_1(\mathbf{x}), f_2(\mathbf{x}), \dots, f_w(\mathbf{x})$ are the equations assembled according to Eqs. (6)–(12), and w is the number of equations. The coefficients of the fundamental solutions are the unknowns, along with the parameters to be estimated. Due to nonlinearity in the fundamental solutions, Eq. (23) consists of a system of nonlinear equations and is solved with the least-squares method. To minimize the norm, two gradient-based local optimization algorithms are used, i.e., Levenberg–Marquardt and trust-region-reflective (Levenberg 1944; Marquardt 1963; Yuan 2000). Both algorithms have been implemented in public-domain optimization solvers. In this work, those implemented in the MATLAB nonlinear solver, *lsqnonlin*, are used (The Mathworks 2012). Moreover, while constraints can be placed on \mathbf{x} (e.g., enforcing positive values for K_s), the optimization algorithms require that an initial guess of \mathbf{x} be provided. The initial guess is assigned a random value that varies within the range of the observed pressure heads. Moreover, because under-determined problems generally yield poor solutions in inverting saturated flow problems (Zhang 2014), the above equation system is over-determined for the problems of this study.

The direct inversion method, by assembling the continuity equations, the data equations, and the constraint equations, yields a system of nonlinear equations whose solution contains both the unknown parameters and the unknown coefficients of the fundamental solutions. This is entirely different from the formulation of the traditional indirect techniques. However,

similar to the indirect techniques, solution of the direct method may suffer ill-posedness when insufficient and/or noisy data are used to condition the inversion. Thus, solution may not exist, solution may not be unique, and solution may be unstable. With sufficient and accurate data which yield exact or over-determined equations, the inverse problem becomes well-posed, leading to fast, stable, and accurate solutions. For example, when inversion is well-posed, experiments with different initial guesses of x generally yield identical results. Moreover, though the inverted unsaturated conductivity is reconstructed as $K(z)$, it can be re-estimated as $K(\psi)$ because $\psi(z)$ is also estimated. When the van Genuchten's model is used, the inverted $K(z)$ is first converted to $K(\psi)$, on which Eq. (4) can be fitted to obtain the van Genuchten parameters, i.e., K_s, β, m, n .

After the inverse solution is found, i.e., both the estimated parameters [or $K(\psi)$] and the recovered pressure head profile $\psi(z)$ throughout the inversion domain, flow boundary conditions can be obtained by sampling the pressure heads at the boundary locations. Similarly, using Eq. (17) (Gardner's) or Eq. (21) (van Genuchten's), the Darcy flux field can be reconstructed piecewise for each inversion grid cell. Here, the inverted boundary conditions are included as part of the recovered $\psi(z)$ and there is no need to deal with them separately. For all the problems presented, measurements (pressure heads or fluxes) are sampled internal to the solution domain, although there are no limitations to the measurement locations, i.e., measurements can certainly be sampled at the boundaries and provided to inversion as a form of data constraint. Under the Dupuit assumption, Jiao and Zhang (2014a) inverted spatially variable recharge rates for unconfined aquifers, which in effect provides the vertical flux (both magnitude and direction) at the water table for unsaturated flow inversion.

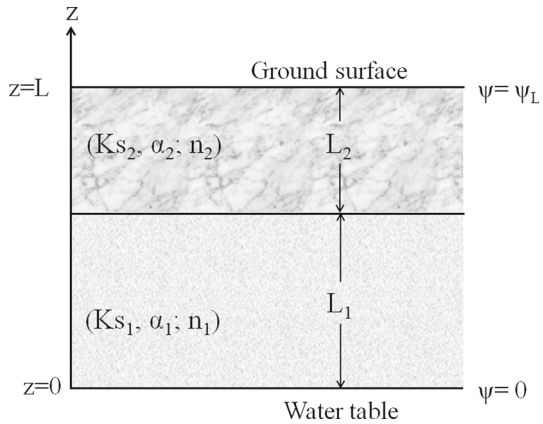
3 Results

To verify the direct method for inverting unsaturated flow, a set of synthetic forward models are created. Parameters, geometry, and boundary conditions of these models are shown in Fig. 1. Each forward model solves Eq. (1) with the finite-difference method subject to a set of appropriately selected BC. These forward models (FDMs) are used to generate a set of synthetic observation data for inversion. For the Gardner's model, 13 FDMs are created. The relevant information is listed in Table 1. For the van Genuchten's model, 7 FDMs are created (see detail below). After simulating the FDM and sampling the appropriate measurements, the inverse method is verified by comparing the estimated parameters, the recovered $K(\psi)$, and the estimated pressure head profile $\psi(z)$ to those of the forward model. For selected cases (both for the Gardner's and for the van Genuchten's models), stability analysis is conducted to evaluate the accuracy of inversion under increasing pressure head measurement errors. In this analysis, pressure heads directly sampled from the FDM are considered error-free. To impose measurement errors, $\psi^m = \psi^{FDM} \pm \Delta\psi$, where ψ^m is measured pressure head provided to inversion, ψ^{FDM} is pressure head sampled from the FDM, and $\Delta\psi$ is a uniform measurement error that is globally unbiased (sum of $\Delta\psi$ over all measurements is 0.0). The highest error imposed is $\pm 10\%$ of the total pressure head variation in the forward model. Inversion results for each model are presented in the following section.

3.1 Gardner's Model

Thirteen forward problems, labeled Cases 1–13, are inverted. Cases 1–6 and 11–13 solve the infiltration problem, while the remaining cases solve flow under evaporation conditions. Table 1 summarizes the observations provided to inversion and the estimated parameters,

Fig. 1 Configuration of the unsaturated flow problem ($L = L_1 + L_2$). Two soil layers are shown: Layer 1 has a thickness of L_1 ; layer 2 has a thickness of L_2



along with domain configuration, true parameters, and BC of the FDM. In simulating the forward models, total domain length ($L_1 + L_2$), K_s , α , and BC are varied systematically to create different flow regimes for inversion. For selected cases, both single- and two-layered problems are simulated. When two layers are modeled, thicknesses of individual layers are also variable. From the FDMs, observations were sampled at regular intervals, while measurement density can vary. The inversion grid has the same domain length as the forward model, although its discretization is much coarser (10 cells). Each inversion grid is discretized uniformly and is the same for all cases.

For Cases 1–10, stability analysis is carried out under increasing measurement errors. Overall, results of this sensitivity analysis suggest that both the variation of $K(\psi)$ and the magnitude of Darcy flux (i.e., infiltration and evaporation rate) control inversion accuracy. Observation sampling density (always sufficiently high to ensure a well-posed inversion) serves to stabilize inversion when measurement errors become large. In the following, the various cases are discussed with more detail.

For Cases 1–4 (infiltration modeling), $L_1 + L_2 = 50$ cm (Table 1). Cases 1 and 2 both have one homogeneous layer. For the range of ψ defined by the forward model, $K(\psi)$ of Case 2 varies by 2 orders of magnitude and but varies less than 1 order for Case 1. Given the same observations (both quantity and locations), inverted parameters of the two cases exhibit nearly identical accuracy when the measurement errors are low (error-free or $\pm 1\%$). When errors are greater ($\pm 10\%$ error), inverted parameters of Case 1 are more accurate compared to those of Case 2. Note that due to the same BC assigned to the forward model, the same relative error (e.g., $\pm 10\%$) yields the same error magnitude for the two cases. As shown in Fig. 2 (a) Case 1 and (c) Case 2, even if the given set of the measured pressure heads are physically unrealistic (i.e., the rough and saw-tooth shape of the head measurement errors with discontinuities), the inversion is able to handle such challenging problems with stable inverted $K(\psi)$ functions for the full range of ψ . Therefore, for the general applications of our approach, we can invert reasonable $K(\psi)$ for any observed pressure heads. Moreover, the inverted $K(\psi)$ and $\psi(z)$ are compared to those of the forward FDM (Fig. 2a–d). For Case 1, the inverted $\psi(z)$ is accurate until error becomes large (at which point $\psi(z)$ exhibits large fluctuations around the true $\psi(z)$ profile), while the inverted $K(\psi)$ is always quite accurate. For Case 2, while $K(\psi)$ exhibits a similar trend as that of Case 1 under increasing errors, the inverted $K(\psi)$ becomes significantly underestimated near the water table when error = $\pm 10\%$. The above results suggest that when observation errors are significant, $K(\psi)$

Table 1 Inverted parameters under increasing measurement errors using the Gardner’s model for Cases 1–13

FDM	Computational domain (cm)	True parameters (subindices indicate the layer number)	True BC (cm)	Flow	Observed data	Inverted parameters
Case 1	$L_1 = 50; L_2 = 0$	$K_s = 9.94; \alpha = 1.4 \times 10^{-2}$	$\psi_0 = 0; \psi_L = -20;$	Infiltr.	20 heads; 1 flux	$K_s = 9.94; \alpha = 1.4 \times 10^{-2}$ (0% error) $K_{s1} = 9.94; \alpha = 1.4 \times 10^{-2}$ ($\pm 1\%$ error) $K_s = 9.79; \alpha = 1.2 \times 10^{-2}$ ($\pm 10\%$ error) $K_s = 296.3; \alpha = 1.26 \times 10^{-1}$ (0% error) $K_s = 289.2; \alpha = 1.24 \times 10^{-1}$ ($\pm 1\%$ error) $K_s = 192; \alpha = 9.53 \times 10^{-2}$ ($\pm 10\%$ error) $K_{s1} = 10; \alpha_1 = 1.5 \times 10^{-2}$ $K_{s2} = 298.9; \alpha_2 = 1.26 \times 10^{-1}$ (0% error) $K_{s1} = 10.1; \alpha_1 = 1.67 \times 10^{-2}$ $K_{s2} = 317.1; \alpha_2 = 1.28 \times 10^{-1}$ ($\pm 1\%$ error) $K_{s1} = 10.6; \alpha_1 = 2.54 \times 10^{-2}$ $K_{s2} = 361; \alpha_2 = 1.34 \times 10^{-1}$ ($\pm 10\%$ error) $K_{s1} = 286.6; \alpha_1 = 1.23 \times 10^{-1}$ $K_{s2} = 9.87; \alpha_2 = 1.38 \times 10^{-2}$ (0% error) $K_{s1} = 311.9; \alpha_1 = 1.31 \times 10^{-1}$ $K_{s2} = 12.9; \alpha_2 = 2.4 \times 10^{-2}$ ($\pm 1\%$ error) $K_{s1} = 525.5; \alpha_1 = 1.77 \times 10^{-1}$ $K_{s2} = 60.4; \alpha_2 = 8.23 \times 10^{-2}$ ($\pm 10\%$ error)
Case 2	$L_1 = 50; L_2 = 0$	$K_s = 297.2; \alpha = 1.26 \times 10^{-1}$	$\psi_0 = 0; \psi_L = -20;$	Infiltr.	20 heads; 1 flux	
Case 3	$L_1 = 25; L_2 = 25$	$K_{s1} = 9.94; \alpha_1 = 1.4 \times 10^{-2}$ $K_{s2} = 297.2; \alpha_2 = 1.26 \times 10^{-1}$	$\psi_0 = 0; \psi_L = -30;$	Infiltr.	20 heads; 1 flux	
Case 4	$L_1 = 25; L_2 = 25$	$K_{s1} = 297.2; \alpha_1 = 1.26 \times 10^{-1}$ $K_{s2} = 9.94; \alpha_2 = 1.4 \times 10^{-2}$	$\psi_0 = 0; \psi_L = -30;$	Infiltr.	20 heads; 1 flux	

Table 1 continued

FDM	Computational domain (cm)	True parameters (subindices indicate the layer number)	True BC (cm)	Flow	Observed data	Inverted parameters
Case 5	$L_1 = 60; L_2 = 40$	$K_{s1} = 297.2; \alpha_1 = 1.26 \times 10^{-1}$ $K_{s2} = 9.94; \alpha_2 = 1.4 \times 10^{-2}$	$\psi_0 = 0; \psi_L = -50;$	Infiltr.	20 heads; 1 flux	$K_{s1} = 312.4; \alpha_1 = 1.27 \times 10^{-1}$ $K_{s2} = 9.94; \alpha_2 = 1.4 \times 10^{-2}$ (0% error) $K_{s1} = 266.7; \alpha_1 = 1.21 \times 10^{-1}$ $K_{s2} = 9.65; \alpha_2 = 1.34 \times 10^{-2}$ ($\pm 1\%$ error) $K_{s1} = 206.9; \alpha_1 = 1.21 \times 10^{-1}$ $K_{s2} = 9.3; \alpha_2 = 1.31 \times 10^{-2}$ ($\pm 5\%$ error)
Case 6	$L_1 = 40; L_2 = 160$	$K_{s1} = 297.2; \alpha_1 = 1.26 \times 10^{-1}$ $K_{s2} = 9.94; \alpha_2 = 1.4 \times 10^{-2}$	$\psi_0 = 0; \psi_L = -80;$	Infiltr.	20 heads; 1 flux	$K_{s1} = 304; \alpha_1 = 1.27 \times 10^{-1}$ $K_{s2} = 9.93; \alpha_2 = 1.4 \times 10^{-2}$ (0% error) $K_{s1} = 263.4; \alpha_1 = 1.2 \times 10^{-1}$ $K_{s2} = 9.48; \alpha_2 = 1.31 \times 10^{-2}$ ($\pm 1\%$ error) $K_{s1} = 173.8; \alpha_1 = 1.16 \times 10^{-1}$ $K_{s2} = 9.04; \alpha_2 = 1.29 \times 10^{-2}$ ($\pm 5\%$ error)
Case 7	$L_1 = 50; L_2 = 0$	$K_s = 9.94; \alpha = 1.4 \times 10^{-2}$	$\psi_0 = 0; \psi_L = -60;$	Evapo.	30 heads; 1 flux	$K_s = 9.92; \alpha = 1.4 \times 10^{-2}$ (0% error) $K_s = 9.83; \alpha = 1.37 \times 10^{-2}$ ($\pm 1\%$ error) $K_s = 9.23; \alpha = 1.17 \times 10^{-2}$ ($\pm 10\%$ error)
Case 8	$L_1 = 50; L_2 = 0$	$K_s = 297.2; \alpha = 1.26 \times 10^{-1}$	$\psi_0 = 0; \psi_L = -60;$	Evapo.	30 heads; 1 flux	$K_s = 293.9; \alpha = 1.26 \times 10^{-1}$ (0% error) $K_s = 261.9; \alpha = 1.23 \times 10^{-1}$ ($\pm 1\%$ error) $K_s = 48.9; \alpha = 8.5 \times 10^{-2}$ ($\pm 10\%$ error)
Case 9	$L_1 = 25; L_2 = 25$	$K_{s1} = 9.94; \alpha_1 = 1.4 \times 10^{-2}$	$\psi_0 = 0; \psi_L = -60;$	Evapo.	30 heads; 1 flux	$K_{s1} = 9.79; \alpha_1 = 1.32 \times 10^{-2}$

Table 1 continued

FDM	Computational domain (cm)	True parameters (subindices indicate the layer number)	True BC (cm)	Flow	Observed data	Inverted parameters
Case 10	$L_1 = 25; L_2 = 25$	$K_{s2} = 297.2; \alpha_2 = 1.26 \times 10^{-1}$ $K_{s1} = 297.2; \alpha_1 = 1.26 \times 10^{-1}$ $K_{s2} = 9.94; \alpha_2 = 1.4 \times 10^{-2}$	$\psi_0 = 0; \psi_L = -60;$	Evapo.	30 heads; 1 flux	$K_{s2} = 292.9; \alpha_2 = 1.26 \times 10^{-1}$ (0% error) $K_{s1} = 8.84; \alpha_1 = 8.81 \times 10^{-3}$ $K_{s2} = 328.5; \alpha_2 = 1.29 \times 10^{-1}$ ($\pm 1\%$ error) $K_{s1} = 293.6; \alpha_1 = 1.25 \times 10^{-1}$ $K_{s2} = 9.87; \alpha_2 = 1.39 \times 10^{-2}$ (0% error) $K_{s1} = 303.3; \alpha_1 = 1.28 \times 10^{-1}$ $K_{s2} = 11; \alpha_2 = 1.64 \times 10^{-2}$ ($\pm 1\%$ error) $K_{s1} = 298.8; \alpha_1 = 1.32 \times 10^{-1}$ $K_{s2} = 13.5; \alpha_2 = 2.13 \times 10^{-2}$ ($\pm 5\%$ error)
Case 11	$L_1 = 200; L_2 = 0$	$K_s = 9.94; \alpha = 1.4 \times 10^{-2}$	$\psi_0 = 0; \psi_L = -100;$	Infiltr.	20 heads; 1 flux	$K_s = 9.94; \alpha = 1.4 \times 10^{-2}$ (0% error)
Case 12	$L_1 = 100; L_2 = 0$	$K_s = 297.2; \alpha = 1.26 \times 10^{-1}$	$\psi_0 = 0; \psi_L = -50;$	Infiltr.	20 heads; 1 flux	$K_s = 300.2; \alpha = 1.26 \times 10^{-1}$ (0% error)
Case 13	$L_1 = 200; L_2 = 0$	$K_s = 297.2; \alpha = 1.26 \times 10^{-1}$	$\psi_0 = 0; \psi_L = -100;$	Infiltr.	20 heads; 1 flux	$K_s = 11.4; \alpha = 9.29 \times 10^{-2}$ (0% error)

FDM domain configuration, true parameters, and BC, and the observations sampled for inversion are shown. For all cases, the number of FDM grid cells is 2000, and the number of inversion grid cells is 10. K_s has a unit of cm/day; α has a unit of cm^{-1}

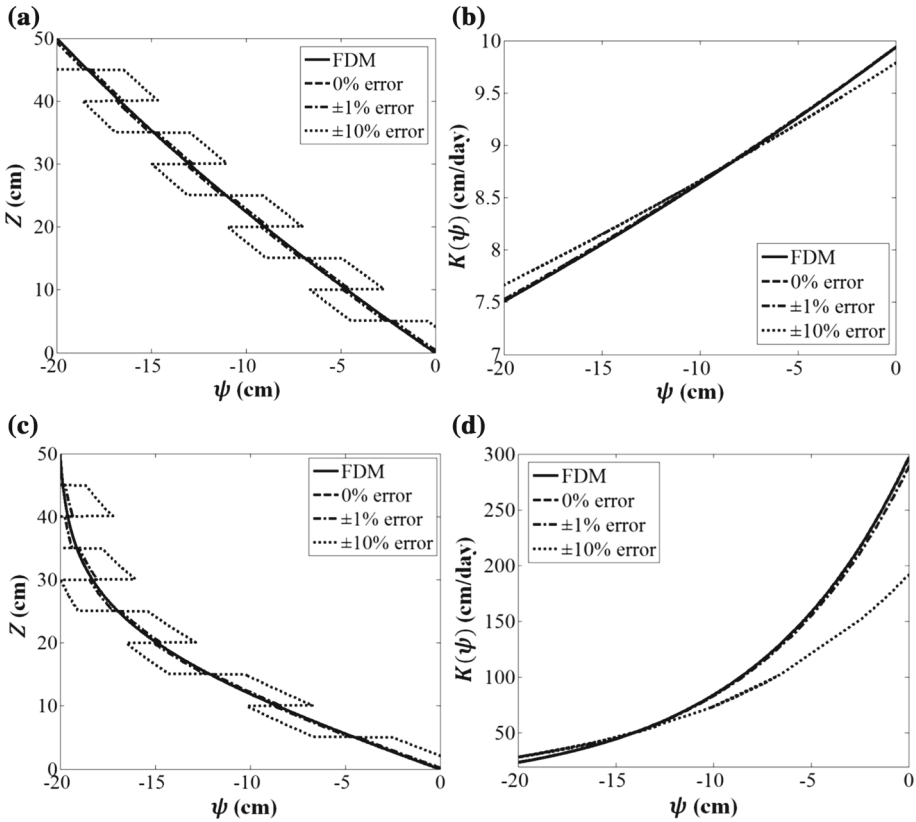


Fig. 2 Gardner’s model. Inversion outcomes of $\psi(z)$ and $K(\psi)$ compared to those of the forward model under infiltration. Case 1 (a, b), Case 2 (c, d)

variation can exert a strong control on inversion accuracy. When $K(\psi)$ is more variable, the forward model is more nonlinear, which poses a greater challenge for the stability of inversion. However, when measurement errors are small, $K(\psi)$ variation has no discernible impact on the quality of inversion.

Keeping the same sampling density and domain length as Cases 1 and 2, Cases 3 and 4 inverted a two-layer model using the parameters of Cases 1 and 2. In Case 3, parameters of Case 1 with a lower $K(\psi)$ variation are assigned to the bottom layer, while parameters of Case 2 with a larger $K(\psi)$ variation are assigned to the top layer (Fig. 1). The opposite configuration is used for Case 4. Overall, inversion results—the estimated K_s , α , $K(\psi)$, $\psi(z)$ (Table 1; Fig. 3 a–d)—are accurate for each layer when measurement errors are small, but become increasingly inaccurate when errors are large. This is similar to what is observed above for one-layer inversion. Moreover, when error is large ($\pm 10\%$), inversion of Case 3 appears more accurate than that of Case 4, suggesting that heterogeneity configuration (where the layer with a higher $K(\psi)$ variation lies) can influence the stability of inversion. Case 3, where the bottom layer has a lower $K(\psi)$ variation, leads to a more stable inversion under increasing measurement errors.

For Cases 5 and 6, the same parameters and sampling density of Case 4 are used, while domain length and BC are modified (Fig. 4a–d). In Case 5, the layer thicknesses are: 40 cm

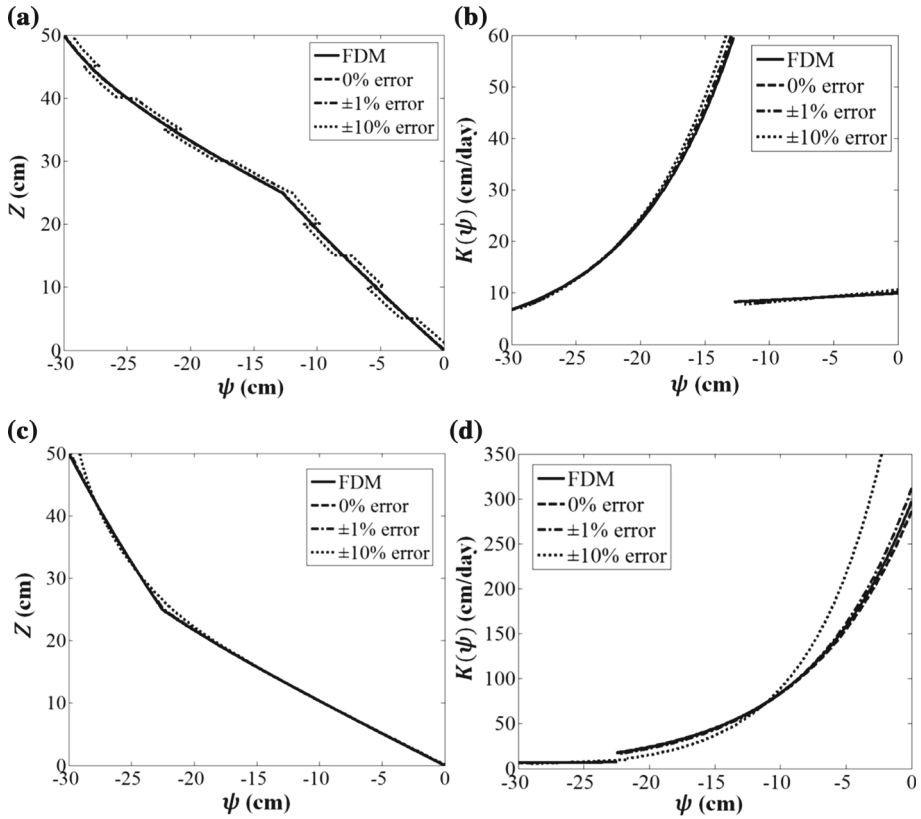


Fig. 3 Gardner's model. Inversion outcomes of $\psi(z)$ and $K(\psi)$ compared to those of the forward model under infiltration. Case 3 (a, b), Case 4 (c, d)

(top) and 60 cm (bottom), for a total length of 100 cm. In Case 6, the thicknesses are: 160 cm (top) and 40 cm (bottom), for a total length of 200 cm. At the land surface, the pressure head (ψ_L) is more negative (-80 cm) in Case 6 compared to that of Case 5 (-50 cm). Because the same layer parameters are assigned, the more negative ψ_L of Case 6 results in a smaller vertical infiltration rate (q_z) compared to that of Case 5. Overall, inversion accuracy is similar to those observed above for Cases 3 and 4, with better accuracy achieved at smaller measurement errors. Given the same error magnitude, inversion outcomes of Case 5 ($L_1 + L_2 = 100$ cm) and Case 6 ($L_1 + L_2 = 200$ cm) do not differ greatly from that of Case 4 ($L_1 + L_2 = 50$ cm), suggesting that domain length does not significantly impact the accuracy and stability of inversion. However, when error is at its highest ($\pm 5\%$), the inverted parameters of Case 6 are less accurate compared to those of Case 5. This is likely due to the smaller infiltration rate in Case 6.

For Cases 7 and 8, the same problems of Cases 1 and 2 are solved except now ψ_L is sufficiently more negative to induce evaporation (Fig. 5a–d). Initially, the same sampling density as that of Cases 1 and 2 is used. However, inversion results are significantly more inaccurate compared to those of Cases 1 and 2. Additional, regularly spaced measurements are then sampled from the forward model until both Cases 7 and 8 reach a similar level of accuracy as Cases 1 and 2. Overall, evaporation is more challenging to invert: To achieve the

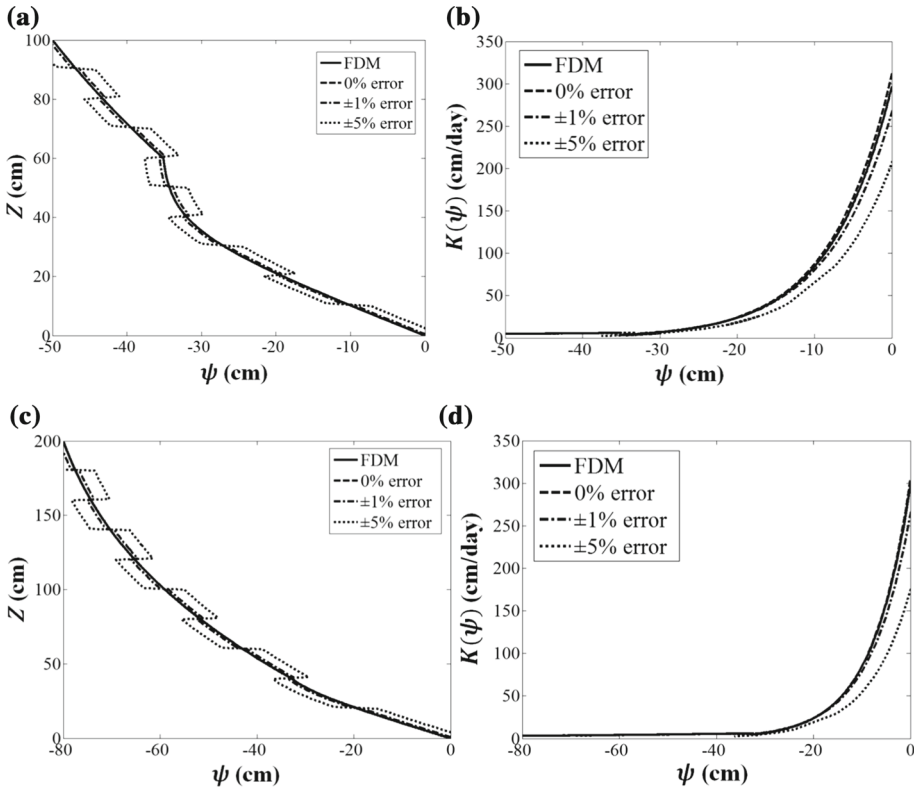


Fig. 4 Gardner’s model. Inversion outcomes of $\psi(z)$ and $K(\psi)$ compared to those of the forward model under infiltration. Case 5 (a, b), Case 6 (c, d)

same accuracy as the infiltration problems, a greater measurement density is needed. This is because, for the same problem configuration, magnitudes of q_z in the evaporation cases are much smaller than those of infiltration.

For Cases 9 and 10, the same problems of Cases 3 and 4 are solved except now ψ_L is sufficiently more negative to induce evaporation (Fig. 6a–d). Again, compared to Cases 3 and 4, a significantly higher sampling density is needed to achieve similar inversion accuracies. When $\pm 5\%$ error is imposed on the measurements, Case 9’s inversion results are quite inaccurate and are excluded. Interestingly, given the same measurement error, results of Case 9 are worse compared to those of Case 10. In the flow fields of Cases 3 and 10 (whose inversions are more accurate compared to Cases 4 and 9, respectively), the layer with a greater $K(\psi)$ variation is first encountered during unsaturated flow.

To investigate the effect of q_z on inversion accuracy, three additional problems are investigated using error-free measurements. Case 11 has the same parameters and sampling density as Case 1, but the domain length and BC are varied: $L_1 + L_2 = 200$ cm and $\psi_L = -100$ cm. The new length and BC give rise to a $q_z = -1.97$ cm/day, which is 3 times smaller than q_z of Case 1 (-5.12 cm/day). The inverted parameters of Case 11 are shown in Table 1, which are identical those of Case 1. The inverted $K(\psi)$ and $\psi(z)$ (not shown) are also close to those of Case 1 as well as the forward model. Similarly, Cases 12 and 13 have the same parameters and sampling density as Case 2, except their domain lengths and BC are modified,

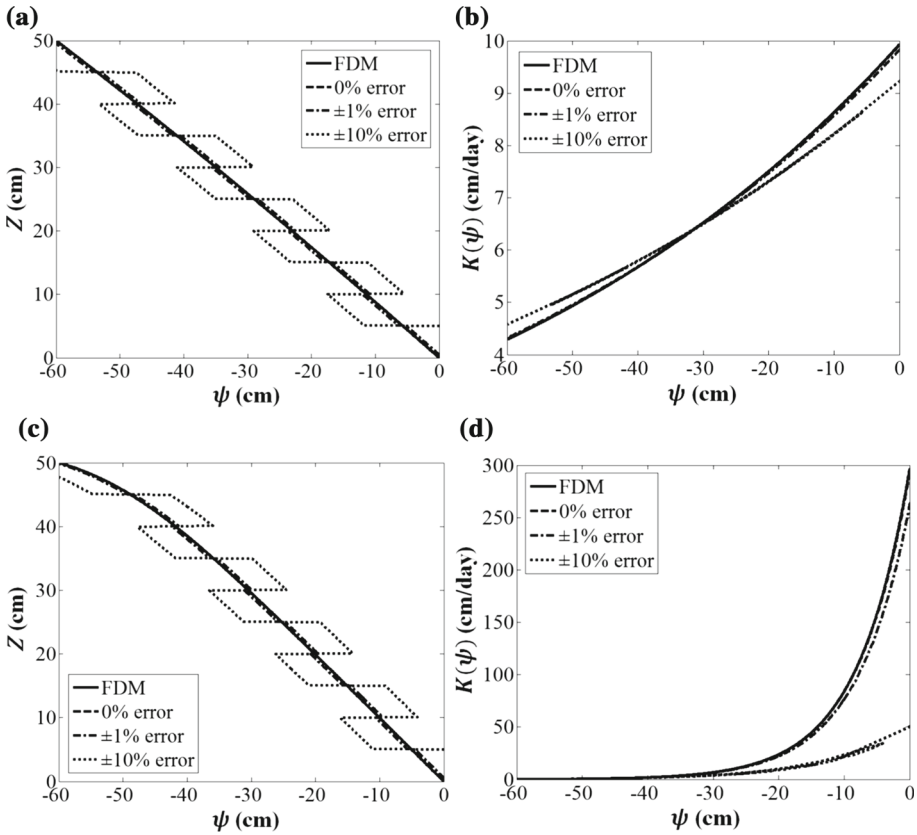


Fig. 5 Gardner’s model. Inversion outcomes of $\psi(z)$ and $K(\psi)$ compared to those of the forward model under evaporation. Case 7 (a, b), Case 8 (c, d)

which give rise to a $q_z = -0.54$ cm/day (Case 12) and -0.001 cm/day (Case 13)—43 and 23,410 times smaller than q_z of Case 2 (-23.41 cm/day), respectively. For Case 12, both the inverted parameters and $K(\psi)$ and $\psi(z)$ (not shown) are close to the forward model. For Case 13, the inverted parameters, particularly K_s , are not accurate, which leads to inaccurate $K(\psi)$ recovery. However, the estimated $\psi(z)$ is very accurate. The above exercise suggests that inversion accuracy is strongly affected by the magnitude of infiltration (or evaporation) rate, which could be explained by the effect of finite arithmetic. Using the Darcy’s law as an example, $K(\psi)$ is estimated by the division of q_z with the hydraulic gradient. Under low flow conditions, both q_z and gradient are small, and $K(\psi)$ becomes less identifiable.

3.2 Van Genuchten’s Model

With the van Genuchten’s model, both infiltration and evaporation ψ are solved in the forward model. Seven cases (Cases 14–20) are inverted. Parameters of the forward model and the inversion outcomes are shown in Table 2 and Figs. 4 and 5. Cases 14–18 solve infiltration, while the remaining cases solve flow under evaporation. In simulating the forward models, K_s , β , m , n , and boundary conditions are varied systematically to create different flow regimes for inversion. The coefficients of van Genuchten’s model are selected from [Carsel](#)

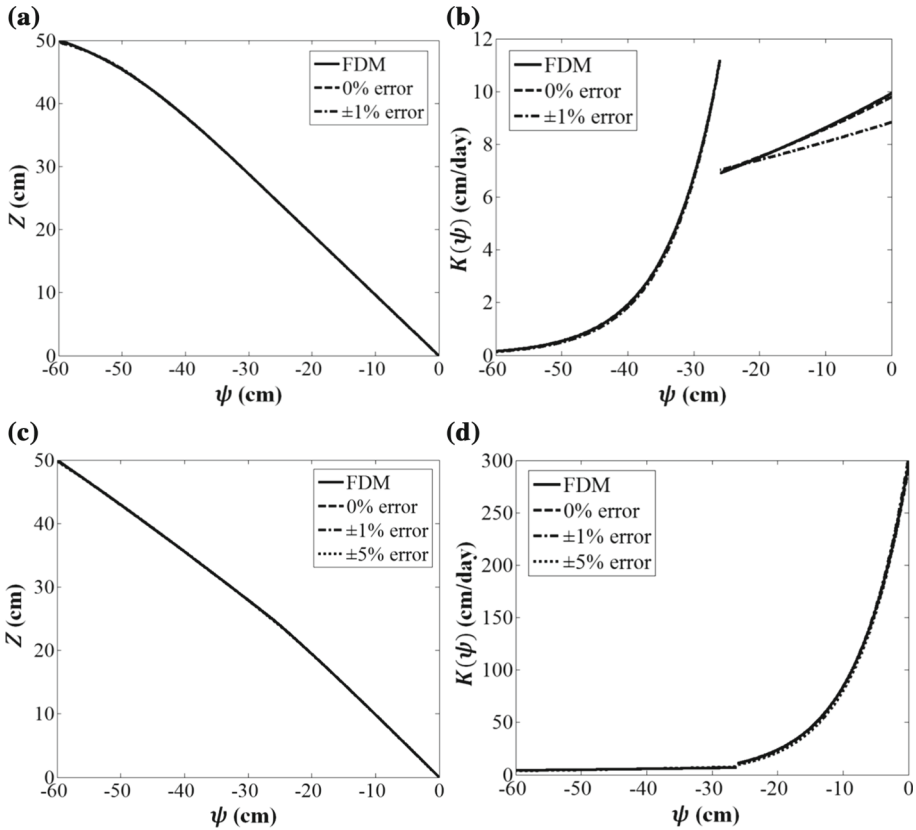


Fig. 6 Gardner’s model. Inversion outcomes of $\psi(z)$ and $K(\psi)$ compared to those of the forward model under evaporation. Case 9 (a, b), Case 10 (c, d)

and Parrish (1988) for different soil textures (Table 2). For some cases, both single- and two-layered problems are investigated. From the FDMs, observations were sampled regularly, while measurement density can vary. The inversion grid has the same domain length as the forward model. Each inversion grid is discretized uniformly.

Under infiltration, Cases 14 and 15 invert a one-layered model under increasing measurement errors, while parameters of “loam” and “sandy clay loam” are assigned to their respective van Genuchten’s model (Carsel and Parrish 1988). The inverted parameters and $\psi(z)$ and $K(\psi)$ are shown in Table 2 and Fig. 7a–d. When error magnitude is low (either error-free or $\pm 1\%$ error), both parameter and state variable estimation are successful. When error increases to $\pm 5\%$, inversion accuracy significantly degrades, particularly in the estimated K_s (β , n estimation are reasonable), which then degrades the estimation of $K(\psi)$. Cases 16–17 invert a similar one-layered problem, although the soil texture has changed to “clay” (Case 16) and “sand” (Case 17). The same BC of Cases 14 and 15 are adopted, while sampling density is slightly increased for Case 17. Compared to the previous soil textures, inverted parameters of the new cases suffer greater inaccuracies even when the same error magnitude is imposed (Fig. 8a–d). In Case 17, when error = $\pm 5\%$, inversion outcomes are physically unreasonable and are excluded. Among the above cases, $K(\psi)$ of Case 17 varies the most (i.e., over 3 orders of magnitude), which likely leads to its observed high sensitivity

Table 2 Inverted parameters under increasing measurement errors using van Genuchten's model for Cases 14–20

FDM	Computational domain (cm)	Soil texture	True parameters (subindices indicate the layer number)	BC (cm)	Flow	Observed data	Inverted parameters
Case 14	$L_1 = 50; L_2 = 0$	Loam	$K_s = 24.96;$ $\beta = 0.036;$ $n = 1.56$	$\psi_0 = 0;$ $\psi_L = -20$	Infiltr.	20 heads; 20 fluxes	$K_s = 23.3; \beta = 0.037;$ $n = 1.6$ (0% error)
Case 15	$L_1 = 50; L_2 = 0$	Sandy clay loam	$K_s = 31.44;$ $\beta = 0.059;$ $n = 1.48$	$\psi_0 = 0;$ $\psi_L = -20$	Infiltr.	20 heads; 20 fluxes	$K_s = 21.2; \beta = 0.037;$ $n = 1.67$ ($\pm 1\%$ error) $K_s = 15.8; \beta = 0.038;$ $n = 1.9$ ($\pm 5\%$ error) $K_s = 33.96; \beta = 0.064;$ $n = 1.49$ (0% error)
Case 16	$L_1 = 50; L_2 = 0$	Clay	$K_s = 4.8;$ $\beta = 0.008;$ $n = 1.09$	$\psi_0 = 0;$ $\psi_L = -20$	Infiltr.	20 heads; 20 fluxes	$K_s = 30.4; \beta = 0.064;$ $n = 1.52$ ($\pm 1\%$ error) $K_s = 14.55; \beta = 0.057;$ $n = 1.88$ ($\pm 5\%$ error) $K_s = 1.29; \beta = 0.014;$ $n = 1.26$ (0% error)
Case 17	$L_1 = 50; L_2 = 0$	Sand	$K_s = 712.8;$ $\beta = 0.145;$ $n = 2.68$	$\psi_0 = 0;$ $\psi_L = -20$	Infiltr.	30 heads; 30 fluxes	$K_s = 0.87; \beta = 0.017;$ $n = 1.37$ ($\pm 1\%$ error) $K_s = 0.56; \beta = 0.019;$ $n = 1.52$ ($\pm 5\%$ error) $K_s = 730.7; \beta = 0.144;$ $n = 2.55$ (0% error) $K_s = 1486.1; \beta = 0.159;$ $n = 2.68$ ($\pm 1\%$ error)

Table 2 continued

FDM domain (cm)	Computational domain (cm)	Soil texture	True parameters (subindices indicate the layer number)	BC (cm)	Flow	Observed data	Inverted parameters
Case 18	$L_1 = 25$; $L_2 = 25$	L_2 : loam; L_1 : sandy clay loam	$K_{s1} = 31.44$; $\beta_1 = 0.059$; $n_1 = 1.48$ $K_{s2} = 24.96$; $\beta_2 = 0.036$; $n_2 = 1.56$	$\psi_0 = 0$; $\psi_L = -30$	Infiltr.	30 heads; 30 fluxes	$K_{s1} = 23.82$; $\beta_1 = 0.061$; $n_1 = 1.62$ $K_{s2} = 27.28$; $\beta_2 = 0.037$; $n_2 = 1.53$ (0% error) $K_{s1} = 18.48$; $\beta_1 = 0.062$; $n_1 = 1.8$ $K_{s2} = 26.1$; $\beta_2 = 0.036$; $n_2 = 1.54$ ($\pm 1\%$ error) $K_{s1} = 14.1$; $\beta_1 = 0.054$; $n_1 = 1.85$ $K_{s2} = 25.6$; $\beta_2 = 0.035$; $n_2 = 1.55$ ($\pm 5\%$ error) $K_{s1} = 34.39$; $\beta_1 = 0.038$; $n_1 = 1.45$ (0% error)
Case 19	$L_1 = 50$; $L_2 = 0$	Loam	$K_s = 24.96$; $\beta = 0.036$; $n = 1.56$	$\psi_0 = 0$; $\psi_L = -60$	Evapo.	30 heads; 30 fluxes	$K_s = 32.52$; $\beta = 0.038$; $n = 1.46$ ($\pm 1\%$ error) $K_s = 25.51$; $\beta = 0.039$; $n = 1.47$ ($\pm 5\%$ error)
Case 20	$L_1 = 25$; $L_2 = 25$	L_2 : loam; L_1 : sandy clay loam	$K_{s1} = 31.44$; $\beta_1 = 0.059$; $n_1 = 1.48$ $K_{s2} = 24.96$; $\beta_2 = 0.036$; $n_2 = 1.56$	$\psi_0 = 0$; $\psi_L = -60$	Evapo.	30 heads; 30 fluxes	$K_{s1} = 40.83$; $\beta_1 = 0.077$; $n_1 = 1.5$ $K_{s2} = 42.46$; $\beta_2 = 0.043$; $n_2 = 1.48$ (0% error) $K_{s1} = 30.81$; $\beta_1 = 0.078$; $n_1 = 1.66$ $K_{s2} = 23.55$; $\beta_2 = 0.037$; $n_2 = 1.77$ ($\pm 1\%$ error)

FDM domain configuration, true parameters, and BC, and the observations sampled for inversion are also shown. For all cases, the number of FDM grid cells is 2000, and the number of inversion grid cells is 10, with the exception of Case 17 for which the inversion grid has 20 cells. K_s has a unit of cm/day; β has a unit of cm^{-1}

to error. Moreover, when measurement error is significant, the inverted $K(\psi)$ of all cases is consistently the least accurate when water table is neared. Inspection of the forward models suggests that $K(\psi)$ often varies the most at such location.

Case 18 solves a two-layered problem using parameters of Case 14 (bottom layer) and Case 15 (top layer). Both measurement density and BC are varied. Compared to Cases 14 and 15, given the same error magnitude, the inverted parameters suffer greater inaccuracies, although the inverted $K(\psi)$ and $\psi(z)$ exhibit similar error behavior (Fig. 9a, b). Overall, similar to the Gardner's model, two-layered problem is more challenging to invert.

Cases 19 and 20 solve evaporation. Case 19 uses the same soil model as Case 14 (with "loam" as the soil texture), except its BC are modified to induce evaporation. Sampling density of Case 19 is increased from that of Case 14 by 50%. However, at every error magnitude, the inverted parameters of Case 19 are less accurate compared to those of Case 14. The recovered state variable (Fig. 10a), however, is not too different from those of Case 14. Case 20 (Fig. 10c, d) solves the same problem as Case 18 (two-layered model), except its BC are modified to induce evaporation. The same sampling density is used. At every error magnitude, the inverted parameters of Case 20 are less accurate compared to those of Case 18, e.g., inversion outcomes become unphysical when error magnitude is $\pm 5\%$, while those of Case 18 are still reasonable. For the same soil regime, again, evaporation is more challenging to invert. Finally, Case 14 is inverted under error-free conditions, but the domain length is extended to 100 cm. Given the same measurement density, inversion accuracy in both the estimated $K(\psi)$ and the recovered pressure head profile is not significantly affected (not shown).

4 Discussion

With the direct method, by establishing continuity, data conditioning, and physical flow constraints in the inversion domain, the unknown unsaturated flow BC are obtained as part of the local pressure head and flux solutions. BC are therefore not formulated as parameters of optimization along with the soil hydraulic properties, which has been attempted by the indirect inversion approaches (e.g., [Scharnagl et al. 2011](#)). The direct method developed and tested for 1D flows thus could be extended to higher spatial dimensions without invoking numerous BC parameters. Moreover, similar to the earlier works on saturated flow inversion, this study has utilized flux measurements to condition inversion, although fluxes can be replaced by flow rates for higher-dimensional problems after an appropriate integration of the flux-based data constraints ([Irsa and Zhang 2012](#)). An advantage of sampling point-scale fluxes is that these measurements can provide local information on pressure head and its gradient, which may facilitate accurate estimation of the local soil water parameters. The theoretical development proposed in this study thus aims to provide an impetus for developing new soil water characterization techniques that will allow accurate sampling of in situ fluxes, which may in turn facilitate the inversion of detailed soil parameters.

For all the problems presented above, the forward model domain extends from the land surface to the water table where $\psi(z = 0) = 0$, and the measurement design follows suite, i.e., pressure heads are sampled regularly from near the land surface to above the water table. All flux measurements are sampled internal to the solution domain. However, the direct inversion method is not constrained by this sampling design. For example, the domain for inversion (i.e., sampling locations) does not need to extend to the land surface or the water table. Inversion can be performed wherever the measurements lie, which can include such

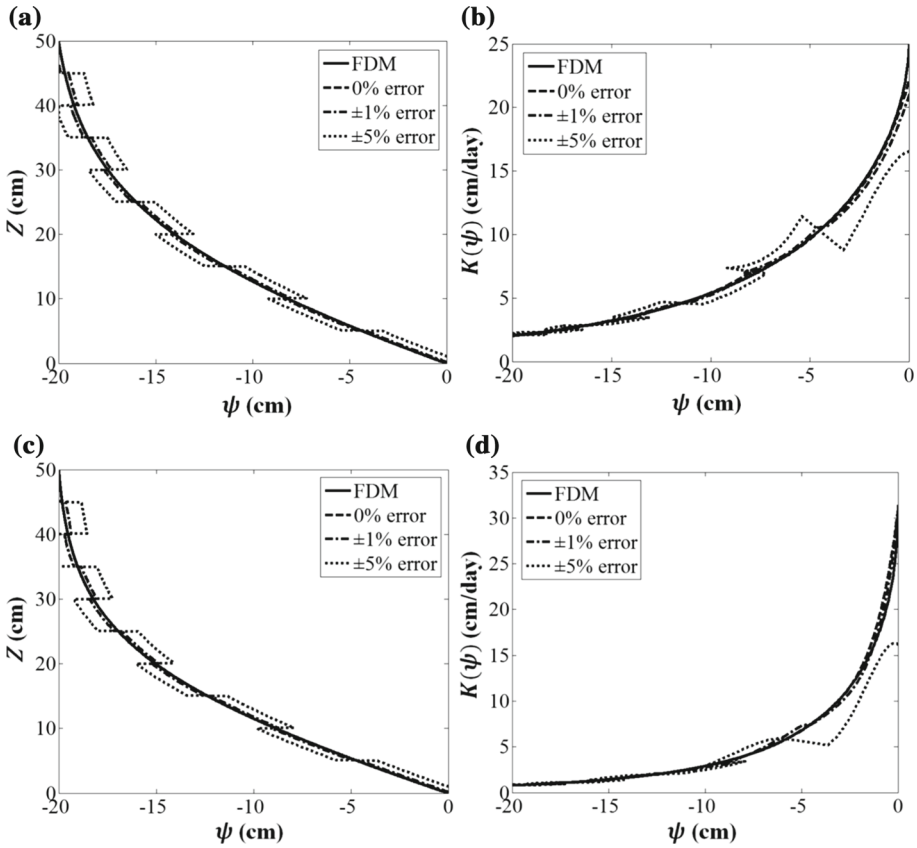


Fig. 7 Van Genuchten’s model. Inversion outcomes of $\psi(z)$ and $K(\psi)$ compared to those of the forward model under evaporation. Case 14 (a, b), Case 15 (c, d)

physical flow boundaries or only be part of the unsaturated zone. In addition, if subsurface flux measurements prove difficult to acquire, the measured water flux can be obtained at the land surface since the flux is the same everywhere for one-dimensional steady-state flow. In this case, the upper inversion domain extends to the land surface where this boundary flux is known as a measurement (the lower boundary location is determined by the deepest measurements which may or may not extend to the water table). To illustrate this, the problem of Case 1 is inverted again using a subdomain spanning a vertical interval of $z = [10, 50]$ cm. From the same interval, which lies 10 cm above the water table, 16 pressure heads and 1 flux were sampled from the forward model. The heads were sampled regularly, while the flux is sampled at $z = 50$ cm (land surface). Figure 11 shows the inverted pressure head and unsaturated conductivity under increasing measurement errors. The behavior of the inverse solution is nearly identical to that of the earlier result when the domain extends to the water table (Fig. 2a, b). Moreover, using the same approach as outlined in this work, variably saturated flow has been successfully inverted for vertical infiltration in a homogeneous soil, where the lower BC have a positive pressure head corresponding to an arbitrary water depth below the water table in the saturated zone. Success of inversion is expected because inversion honors continuity and physics of flow during such flow processes. Future research will explore inversion under variably saturated conditions for heterogeneous soils.

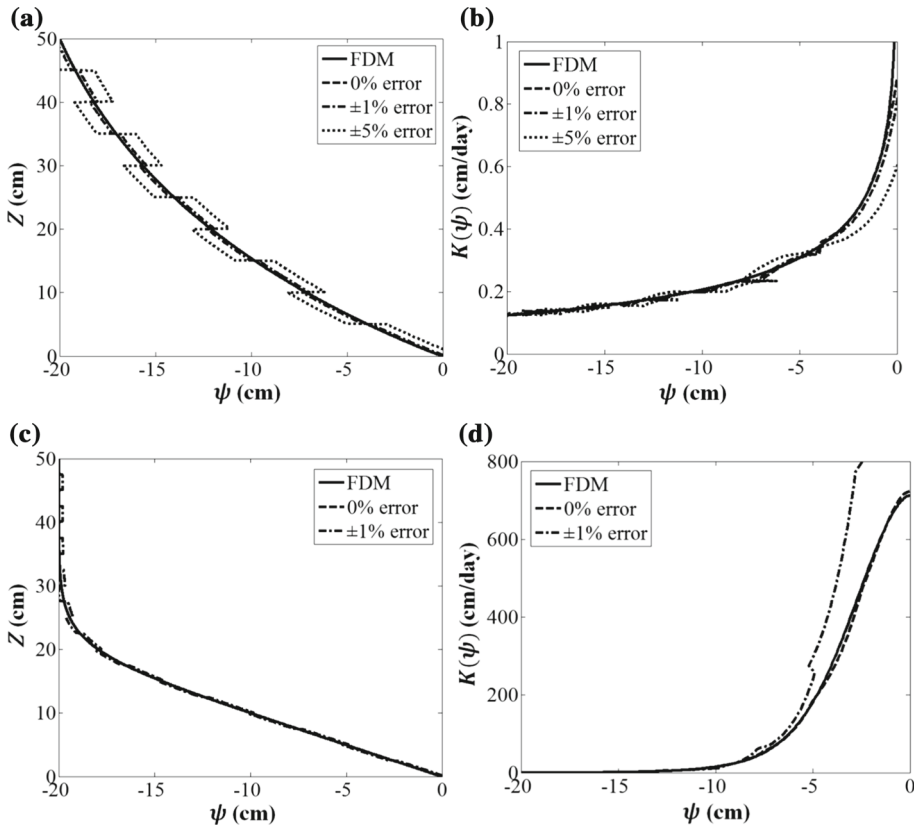


Fig. 8 Van Genuchten's model. Inversion outcomes of $\psi(z)$ and $K(\psi)$ compared to those of the forward model under evaporation. Case 16 (a, b), Case 17 (c, d)

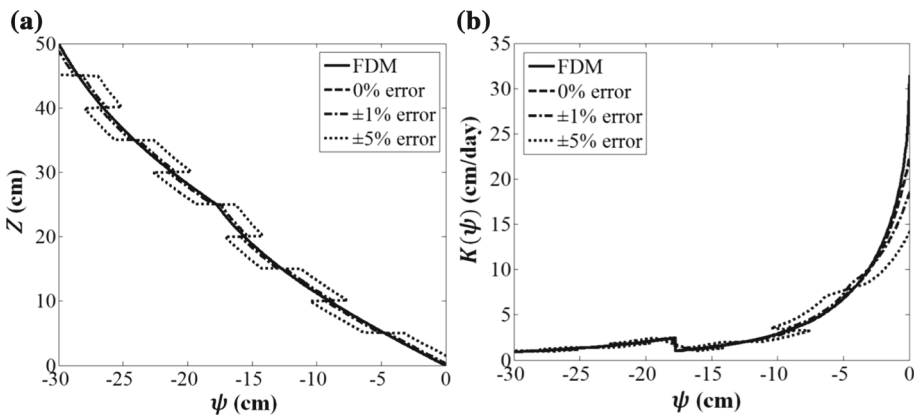


Fig. 9 Van Genuchten's model. Inversion outcomes of $\psi(z)$ and $K(\psi)$ compared to those of the forward model under evaporation. Case 18 (a, b)

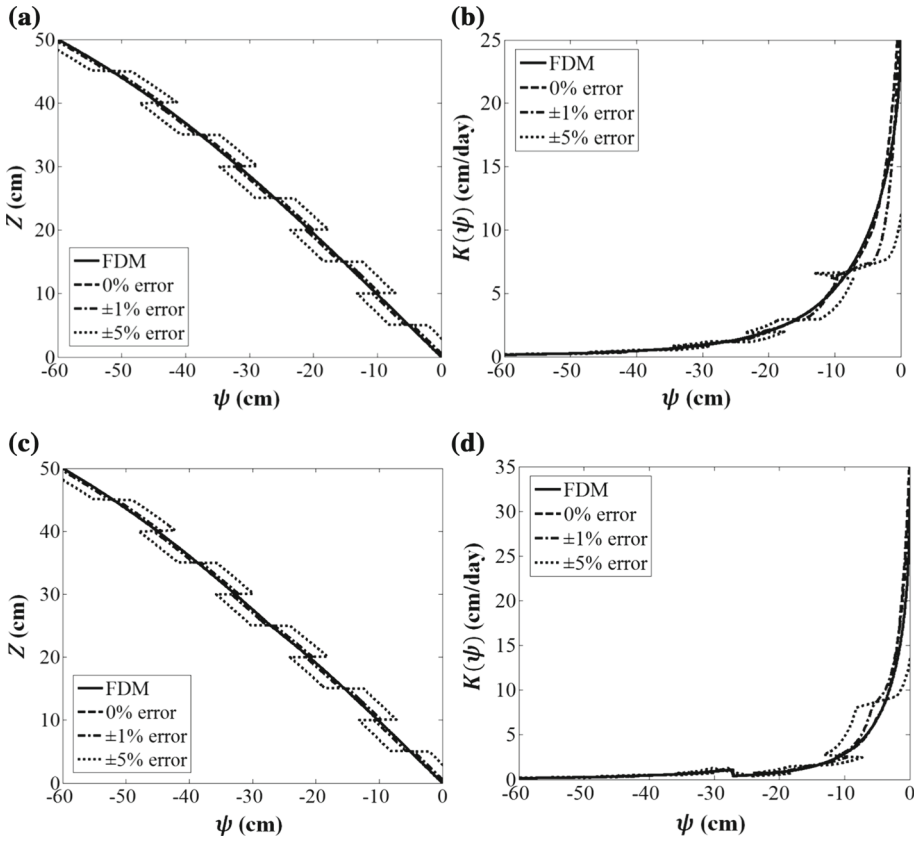


Fig. 10 Van Genuchten's model. Inversion outcomes of $\psi(z)$ and $K(\psi)$ compared to those of the forward model under evaporation. Case 19 (a, b), Case 20 (c, d)

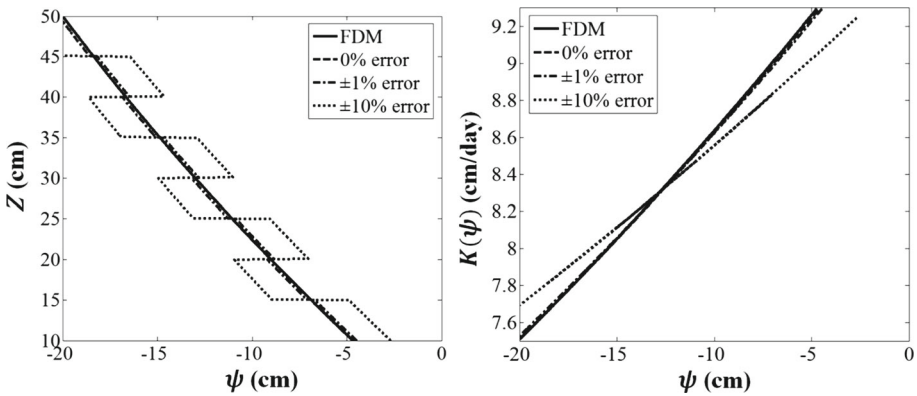


Fig. 11 Gardner's model. Inversion outcomes of $\psi(z)$ and $K(\psi)$ compared to those of the forward model under infiltration for a subdomain of Case 1

For both the Gardner and the van Genuchten models, the proposed second-order approximate solution of $\psi(z)$ reflects the common use of second-order polynomials as local interpolation functions for solving partial differential equations with the finite element method. A linearly weighted function, constructed using these interpolation functions, is a second-order polynomial and is used to approximate the state variable (e.g., pressure head) in developing the finite element solution of the forward model (Zhang et al. 2006). In its weak formulation, second-order polynomials can be implemented using simple elements; thus, they are considered more desirable compared to higher-order polynomials (Bear and Cheng 2010). In the inversion, however, higher-order polynomials can certainly be used based on which continuity on the gradient of fluxes can also be added as constraints. While seeking a physical basis for these local solutions (e.g., by examining laboratory data), higher-order local solutions will be investigated in the future.

Finally, this study investigates well-posed problems where flux measurements are used to constrain the unsaturated K estimation. By examining the Darcy's law, unique estimation of the unsaturated K requires both pressure head and flux measurements. This is because physically it is possible that two identical pressure distributions can correspond to different unsaturated K s for different soil water velocities. Fluxes here are assumed to be continuum properties, and by considering only vertical flow, flux variation in the lateral direction is ignored. The soil media are considered to be either homogeneous or layered, for which fluxes can be obtained from flow rates measured over given areas. Though such measurements are not commonly taken in the field, recent advances in velocity measurement for the saturated zones (Labaky et al. 2009) may point to the development of such technology for soil studies. Moreover, because moisture content data are frequently collected in the field, future work will extend the inversion by conditioning to such data.

5 Conclusion

To invert steady-state infiltration and evaporation in the vadose zone when soil hydraulic boundary conditions are unknown, this study develops a direct inversion method to simultaneously estimate the unsaturated flow parameters (both of the Gardner and the van Genuchten models) and the state variables (pressure head profile) which include the unknown boundary pressure heads. Unlike the objective function-based indirect inversion techniques, the direct method does not require forward flow simulations to assess measurement-to-model fit; thus, the knowledge of model boundary conditions is not required. Instead, the method employs a set of local approximate solutions (LAS) of flow to impose continuity of pressure head and soil water fluxes throughout the solution domain, which are then conditioned by measurements. The proposed direct method can reduce nonuniqueness often encountered in the traditional inverse methods. Without the need of iterations which are part of the optimization and parameter search algorithms in the traditional methods, the approach proposed in this study can significantly reduce the computational burden. Because these LAS are not exact, a set of equation constraints is needed, which enforces flow physics at selected spatial locations. Success of direct inversion is demonstrated by inverting vertical infiltration and evaporation in various soil types with homogeneous or layered heterogeneity. Several conclusions are obtained based on the results of this study:

1. Given sufficient measurements, inversion yields a well-posed system of nonlinear equations that can be solved in one step with optimization. The method is thus computationally efficient without the need to repeatedly run forward simulation model.

2. Given error-free measurements, pressure heads, soil hydraulic parameters, and a nonparametric unsaturated conductivity function can be accurately recovered. When measurement errors are increased, estimation of parameters and pressure head becomes less accurate, but the inverse solution is still stable, i.e., estimation errors remain bounded.
3. For inverting unsaturated flows with the Gardner's and the van Genuchten's models, difficulty in inversion increases with (1) decreasing infiltration or evaporation rate, (2) increasing variation of the unsaturated conductivity, (3) change in flow direction (i.e., infiltration is easier to invert than evaporation), and (4) increasing number of soil layers. Overall, for a fixed problem setup (i.e., domain length, BC, unsaturated conductivity, sampling density and measurement error, flow direction), the van Genuchten model is more challenging to invert. For both soil water models, increasing domain length does not appear to play a significant role on either inversion accuracy or its stability.

In this work, it is known from the inverted results that when the magnitude of Darcy flux is very small, convergence can become an issue in inversion, for both infiltration and evaporation, and for both Gardner and van Genuchten's models. Future work will address inversion of spatially correlated heterogeneity in the unsaturated parameters. Transient inversion will be attempted, whereas time-dependent data may provide additional constraints for parameter and state estimation. For sites lacking characterization data, effective parameters and functions will be examined. For such cases, preliminary results with the Gardner's model have led to encouraging outcomes. For example, when soil interface is unknown, effective functions are successfully inverted while accurately capturing the pressure head profile.

Acknowledgements This work is supported by the University of Wyoming Center for Fundamentals of Sub-surface Flow of the School of Energy Resources (WYDEQ49811ZHNG) and NSF EPSCoR (EPS 1208909).

References

- Bear, J., Cheng, A.H.D.: Modeling Groundwater Flow and Contaminant Transport. Springer, Berlin (2010)
- Bohne, K., Roth, C., Leij, F.J., van Genuchten, M.T.: Rapid method for estimating the unsaturated hydraulic conductivity from infiltration measurements. *Soil Sci.* **155**(4), 237–244 (1993)
- Brouwer, G.K., Fokker, P.A., Wilschut, F., Zijl, W.: A direct inverse model to determine permeability fields from pressure and flow rate measurements. *Math. Geosci.* **40**(8), 907–920 (2008)
- Carrera, J., Neuman, S.P.: Estimation of aquifer parameters under steady-state and transient condition: 2. Uniqueness, stability, and solution algorithms. *Water Resour. Res.* **22**(2), 211–227 (1986)
- Carsel, R.F., Parrish, R.S.: Developing joint probability distributions of soil water retention characteristics. *Water Resour. Res.* **24**(5), 755–769 (1988)
- Crescimanno, G., Iovino, M.: Parameter estimation by inverse method based on one-step and multi-step outflow experiments. *Geoderma* **68**, 257–277 (1995)
- Dai, Z., Samper, J.: Inverse problem of multicomponent reactive chemical transport in porous media: formulation and applications. *Water Resour. Res.* **40**, W07407 (2004). doi:[10.1029/2004WR003248](https://doi.org/10.1029/2004WR003248)
- Dai, Z., Samper, J., Wolfsberg, A., Levitt, D.: Identification of relative conductivity models for water flow and solute transport in unsaturated compacted bentonite. *Phys. Chem. Earth* **33**, S177–S185 (2008). doi:[10.1016/j.pce.2008.10.012](https://doi.org/10.1016/j.pce.2008.10.012)
- Dirksen, C.: Unsaturated hydraulic conductivity. In: Mullins, C.E., Smith, K.A. (eds.) *Soil and Environmental Analysis: Physical Methods, Revised, and Expanded*, pp. 183–237. CRC Press, Boca Raton (2000)
- Durner, W., Lipsius, K.: Determining soil hydraulic properties. In: Anderson, M.G. (ed.) *Encyclopedia of Hydrological Sciences*, chap. 75, Wiley, Chichester, pp. 1121–1143. doi:[10.1002/0470848944.hsa077b](https://doi.org/10.1002/0470848944.hsa077b) (2005)
- Durner, W., Schultze, E.B., Zurmühl, T.: State-of-the-art in inverse modeling of inflow/outflow experiments. Characterization and measurement of the hydraulic properties of unsaturated porous media, pp. 661–681. In: van Genuchten, M.T., Leij, F.J., Wu, L. (eds.) *Proceedings of International Workshop*. CA. October 22–24, Riverside (1997)

- Eching, S.O., Hopmans, J.W.: Optimization of hydraulic functions from transient outflow and soil water pressure data. *Soil Sci. Soc. Am. J.* **57**(5), 1167–1175 (1993)
- Fairweather, G., Karageorghis, A.: The method of fundamental solutions for elliptic boundary value problems. *Adv. Comput. Math.* **9**(1–2), 69–95 (1998)
- Gardner, W.: Some steady-state solutions of the unsaturated moisture flow equation with application to evaporation from a water table. *Soil Sci.* **85**, 228–232 (1958)
- Hastings, W.K.: Monte Carlo sampling methods using Markov chains and their applications. *Biometrika* **57**, 97–109 (1970). doi:[10.1093/biomet/57.1.97](https://doi.org/10.1093/biomet/57.1.97)
- Hill, M.C., Tiedeman, C.R.: *Effective groundwater model calibration: with analysis of data, sensitivities, predictions, and uncertainty*. Wiley-Interscience, New York (2007)
- Irsa, J., Zhang, Y.: A new direct method of parameter estimation for steady state flow in heterogeneous aquifers with unknown boundary conditions. *Water Resour. Res.* **48**(W09), 526 (2012). doi:[10.1029/2011WR011756](https://doi.org/10.1029/2011WR011756)
- Ines, A.V.M., Mohanty, B.P.: Near-surface soil moisture assimilation to quantify effective soil hydraulic properties using genetic algorithm. I. Conceptual modeling. *Water Resour. Res.* **44**, W06422 (2008). doi:[10.1029/2007WR005990](https://doi.org/10.1029/2007WR005990)
- Jiao, J.Y., Zhang, Y.: Two-dimensional inversion of confined and unconfined aquifers under unknown boundary condition. *Adv. Water Resour.* **65**, 43–57 (2014a)
- Jiao, J.Y., Zhang, Y.: A method based on local approximate solutions (LAS) for inverting transient flow in heterogeneous aquifer. *J. Hydrol.* **514**, 145–149 (2014b)
- Jiao, J.Y., Zhang, Y.: Tensor hydraulic conductivity estimation for heterogeneous aquifers under unknown boundary conditions. *Groundwater* **53**, 293–304 (2015a). doi:[10.1111/gwat.12202](https://doi.org/10.1111/gwat.12202)
- Jiao, J.Y., Zhang, Y.: Functional parameterization for hydraulic conductivity inversion with uncertainty quantification. *Hydrogeol. J.* **23**, 597–610 (2015b). doi:[10.1007/s10040-014-120205](https://doi.org/10.1007/s10040-014-120205)
- Jiao, J., Zhang, Y.: Direct method of hydraulic conductivity structure identification for subsurface transport modeling. *J. Hydrol. Eng.* **21**(10), 04016033 (2016). doi:[10.1061/\(ASCE\)HE.1943-5584.0001410](https://doi.org/10.1061/(ASCE)HE.1943-5584.0001410)
- Kool, J.B., Parker, J.C.: Analysis of the inverse problem for transient unsaturated flow. *Water Resour. Res.* **24**(6), 817–830 (1988)
- Kool, J.B., Parker, J.C., van Genuchten, MTh: Determining soil hydraulic properties from one-step outflow experiments by parameter estimation: I. Theory and numerical studies. *Soil Sci. Soc. Am. J.* **49**, 1348–1354 (1985a)
- Kool, J.B., Parker, J.C., van Genuchten, MTh: Determining soil hydraulic properties from one-step outflow experiments by parameter estimation: II. Experimental studies. *Soil Sci. Soc. Am. J.* **49**, 354–359 (1985b)
- Labaky, W., Devlin, J.F., Gillham, R.W.: Field comparison of the point velocity probe with other groundwater velocity measurement method. *Water Res. Res.* **45**: W00D30 (2009). doi:[10.1029/2008WR007066](https://doi.org/10.1029/2008WR007066)
- Levasseur, S., Malecot, Y., Boulon, M., Flavigny, E.: Statistical inverse analysis based on genetic algorithm and principal component analysis: method and developments using synthetic data. *Int. J. Numer. Anal. Methods Geomech.* **33**(12), 1485–1511 (2009)
- Levenberg, K.: A method for the solution of certain non-linear problems in least squares. *Q. Appl. Math.* **2**, 164–168 (1944)
- Marquardt, D.W.: An algorithm for least-squares estimation of nonlinear parameters. *J. Soc. Ind. Appl. Math.* **11**(2), 431–441 (1963)
- Mertens, J., Madsen, H., Kristensen, M., Jacques, D., Feyen, J.: Sensitivity of soil parameters in unsaturated zone modelling and the relation between effective, laboratory and in situ estimates. *Hydrol. Process.* **19**, 1611–1633 (2005). doi:[10.1002/hyp.5591](https://doi.org/10.1002/hyp.5591)
- Metropolis, N., Rosenbluth, A.W., Rosenbluth, M.N., Teller, A.H., Teller, E.: Equation of state calculations by fast computing machines. *J. Chem. Phys.* **21**, 1087–1092 (1953)
- Nasta, P., Huynh, S., Hopmans, J.W.: Simplified multistep outflow method to estimate unsaturated hydraulic functions for coarse-textured soils. *Soil Sci. Soc. Am. J.* **75**, 418–425 (2011). doi:[10.2136/sssaj2010.0113](https://doi.org/10.2136/sssaj2010.0113)
- Pasquier, P., Marcotte, D.: Steady-and transient-state inversion in hydrogeology by successive flux estimation. *Adv. Water Resour.* **29**(12), 1934–1952 (2006)
- Ponzini, G., Crosta, G.: The comparison model method: a new arithmetic approach to the discrete inverse problem of groundwater hydrology. *Transp. Porous Media* **3**(4), 415–436 (1988)
- Simunek, J.R., Jaramillo, R.A., Schaap, M.G., Vandervaere, J.P., van Genuchten, MTh: Using an inverse method to estimate the hydraulic properties of crusted soils from tension disc infiltrometer data. *Geoderma* **86**, 61–81 (1998)
- Scharnagl, B., Vrugt, J.A., Vereecken, H., Herbst M.: Inverse modelling of in situ soil water dynamics: investigating the effect of different prior distributions of the soil hydraulic parameters. *Hydrol. Earth Syst.*

- Sci. **15**, 3043–3059. <https://www.hydrol-earth-syst-sci.net/15/3043/2011/>. doi:10.5194/hess-15-3043-2011 (2011)
- Shin, Y., Mohanty, B.P., Ines, A.V.M.: Estimating effective soil hydraulic properties using spatially distributed soil moisture and evapotranspiration products at multiple scales. *Vadose Zone J.* **12**, 1–16 (2013). doi:10.2136/vzj2012.0094
- Sun, N.Z.: *Inverse Problems in Groundwater Modeling*, vol. 364. Kluwer Academic Publishers, Netherlands (1994)
- To-Viet, N., Min, T.-K., Shin, H.: Using inverse analysis to estimate hydraulic properties of unsaturated sand from one-dimensional outflow experiments. *Eng. Geol.* **164**, 163–171 (2013). doi:10.1016/j.enggeo.2013.07.005
- Toorman, A.F., Wierenga, P.J., Hills, R.G.: Parameter estimation of hydraulic properties from one-step outflow data. *Water Resour. Res.* **28**(11), 3021–3028 (1992)
- Van Dam, J.C., Stricker, J.N.M., Verhoef, A.: Inverse method for determining soil hydraulic functions from one-step outflow experiments. *Soil Sci. Soc. Am. J.* **56**, 1042–1050 (1992)
- Van Genuchten, M.T.: A closed-form equation for predicting the hydraulic conductivity of unsaturated soils. *Soil Sci. Soc. Am. J.* **44**(5), 892–898 (1980)
- Vassena, C., Giudici, M., Ponzini, G., Parravicini, G., Meles, G.A.: Tomographic approach to identify transmissivity with differential system method. *J. Hydrol. Eng.* **12**(6), 617–625 (2007)
- Vrugt, J.A., Stauffer, P.H., Wohling, T., Robinson, B.A., Vesselinov, V.V.: Inverse modeling of subsurface flow and transport properties: a review with new developments. *Vadose Zone J.* **7**, 843–864 (2008)
- Yang, C., Dai, Z., Romanak, K., Hovorka, S., Trevino, R.: Inverse modeling of water-rock-CO₂ batch experiments: implications for potential impacts on groundwater resources at carbon sequestration sites. *Environ. Sci. Technol.* **48**(5), 2798–2806 (2014)
- Ye, M., Neuman, S.P., Meyer, P.D., Pohlmann, K.F.: Sensitivity analysis and assessment of prior model probabilities in MLBMA with application to unsaturated fractured tuff. *Water Resour. Res.* **41**, W12429 (2005). doi:10.1029/2005WR004260
- Yuan, Y.: A review of trust region algorithms for optimization. In: *ICIAM 99: Proceedings of the Fourth International Congress on Industrial and Applied Mathematics*, Edinburgh, Oxford University Press, USA (2000)
- Zhang, Y.: Nonlinear inversion of an unconfined aquifer: simultaneous estimation of heterogeneous hydraulic conductivities, recharge rates, and boundary conditions. *Transp. Porous Media* **102**, 275–299 (2014). doi:10.1007/s11242-014-0275-x
- Zhang, Z.F., Ward, A.L., Gee, G.W.: Estimating soil hydraulic parameters of a field drainage experiment using inverse techniques. *Vadose Zone J.* **2**, 201–211 (2003)
- Zhang, Y., Gable, C.W., Person, M.: Equivalent hydraulic conductivity of an experimental stratigraphy—implications for basin-scale flow simulations. *Water Resour. Res.* **42**, W05404 (2006). doi:10.1029/2005WR004720
- Zhang, Y., Irsa, J., Jiao, J.Y.: Three-dimensional aquifer inversion under unknown boundary conditions. *J. Hydrol.* **509**, 416–429 (2014). doi:10.1016/j.jhydrol.2013.11.024
- Zhou, H., Gomez-Hernandez, J.J., Li, L.: Inverse methods in hydrogeology: evolution and recent trends. *Adv. Water Resour.* **63**, 22–37 (2014)